

Deep-Elastic pp Scattering at LHC from Low-x Gluons

M. M. Islam^a, J. Kašpar^{b,c}, R. J. Luddy^d

^a*Department of Physics, University of Connecticut, Storrs, CT 06269, USA (islam@phys.uconn.edu)*

^b*TOTEM Collaboration, CERN, Geneva, Switzerland (Jan.Kaspar@cern.ch)*

^c*Institute of Physics, Academy of Sciences of the Czech Republic, Prague*

^d*Department of Physics, University of Connecticut, Storrs, CT 06269, USA (rjluddy@phys.uconn.edu)*

Abstract

Deep-elastic pp scattering at c.m. energy 14 TeV at LHC in the momentum transfer range $4 \text{ GeV}^2 \lesssim |t| \lesssim 10 \text{ GeV}^2$ is planned to be measured by the TOTEM group. We study this process in a model where the deep-elastic scattering is due to a single hard collision of a valence quark from one proton with a valence quark from the other proton. The hard collision originates from the low-x gluon cloud around one valence quark interacting with that of the other. The low-x gluon cloud can be identified as color glass condensate and has size $\approx 0.3 \text{ F}$. Our prediction is that pp $d\sigma/dt$ in the large $|t|$ region decreases smoothly as momentum transfer increases. This is in contrast to the prediction of pp $d\sigma/dt$ with visible oscillations and smaller cross sections by a large number of other models.

PACS: 12.39.-x; 13.85.Dz; 14.20.Dh

Keywords: pp scattering; LHC/TOTEM; Proton structure; Low-x gluons; Color Glass Condensate

A major discovery from deep-inelastic ep scattering at HERA is the dramatic increase of low-x gluon density in a proton [1]. The HERA data have been well described by the saturation model of Golec-Biernat and Wüsthoff (GBW model)[2]. The prediction of geometric scaling in this model for low-x region ($x < 0.01$) has been impressively confirmed by Stašo et al.[3]. In GBW model, the virtual photon splits into a dipole (a $q\bar{q}$ pair) and the low-x gluons of a proton present an effective black disk to the dipole in the transverse b -plane. In this paper, we present results of our investigation of deep-elastic pp scattering at LHC using key premises of GBW model pertaining to the low-x gluons.

pp elastic scattering at LHC at center of mass energy 14 TeV and momentum transfer range $|t| \approx 0 - 10 \text{ GeV}^2$ is planned to be measured by the TOTEM group [4,5]. By deep-elastic pp scattering — we mean elastic $d\sigma/dt$ distribution in the momentum transfer range $4 \text{ GeV}^2 \lesssim |t| \lesssim 10 \text{ GeV}^2$. In this range, a proton probes the other proton at a transverse distance $b \sim q^{-1}$ ($q = \sqrt{|t|}$) and therefore at distances of one tenth of a fermi (F) or smaller. High energy pp elastic scattering has been studied by us in a model of proton where the proton has an outer cloud of $q\bar{q}$ condensed ground state (size $\approx 0.86 \text{ F}$), an inner shell of baryonic charge density (size $\approx 0.44 \text{ F}$) and an inner core of valence quarks (size $\approx 0.2 \text{ F}$) (Fig. 1) [6]. Large $|t|$ pp elastic scattering in this model is due to a hard collision between a valence quark from one proton with a valence quark from the other proton — where the collision carries off the whole momentum transfer $|t|$ (Fig. 2). In a previous paper, we have studied the case where this collision is due to a hard pomeron (a BFKL pomeron plus its next to leading order corrections) [7]. We now want to study the case where the low-x gluon cloud of one valence quark interacts with that of the other valence quark leading to the deep-elastic scattering.

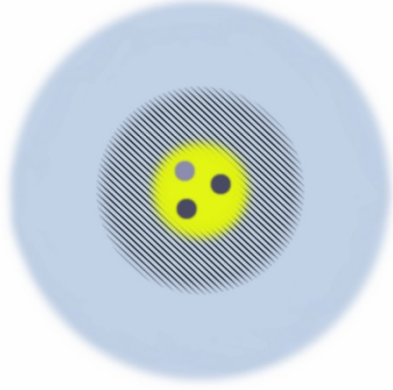


Fig. 1. Model of proton structure underlying our study of high energy pp elastic scattering: proton has an outer cloud of $q\bar{q}$ condensed ground state, an inner shell of baryonic charge density and an inner core of valence quarks.

The valence quarks in our model are color neutral quasi-quarks, because of the gluon clouds around them. To describe the valence quark-quark (q-q) scattering, we consider an eikonal description for a purely absorptive process where the scattering amplitude is given by

$$\hat{T}(\hat{s}, t) = i \hat{p} \hat{W} \frac{1}{2\pi} \int d^2b e^{i \vec{b} \cdot \vec{q}} [1 - \exp(-\hat{\chi}_1(\hat{s}, b))]; \quad (1)$$

$\chi_1(\hat{s}, b)$ is the imaginary part of the eikonal and the hat (^) refers to valence quark-quark scattering. Considering the forward amplitude ($q = 0$) and using the optical theorem: $Im \hat{T}(\hat{s}, 0) = (\hat{p} \hat{W} / 4 \pi) \sigma_{tot}(\hat{s})$, we find

$$\hat{\sigma}_{tot}(\hat{s}) = 2 \int d^2b [1 - \exp(-\hat{\chi}_1(\hat{s}, b))]. \quad (2)$$

In Born approximation, i.e. for single scattering, the corresponding cross section is

$$\hat{\sigma}_B(\hat{s}) = 2 \int d^2b \hat{\chi}_1(\hat{s}, b). \quad (3)$$

If $\hat{\chi}_1(\hat{s}, b)$ is written as $\hat{\chi}_1(\hat{s}, b) = \hat{\sigma}_B(\hat{s}) \frac{1}{2} F(b)$ by introducing a transverse space b -dependence, then from Eq. (3) $\int d^2b F(b) = 1$, and Eq. (2) becomes

$$\hat{\sigma}_{tot}(\hat{s}) = 2 \int d^2b [1 - \exp(-\hat{\sigma}_B(\hat{s}) \frac{1}{2} F(b))]. \quad (4)$$

With the above eikonal framework as our backdrop, let us examine the GBW model. In this model, the total cross section due to a dipole traversing the low- x gluon cloud of a proton is

$$\sigma_{tot}^{dipole}(x, r^2) = 2 \int d^2b [1 - \exp(-r^2 \frac{\pi^2}{3} \alpha_s x g(x, \mu^2) \frac{1}{2} f(b))], \quad (5)$$

where $f(b)$ represents the gluon distribution in the b -plane ($\int d^2b f(b) = 1$). GBW next introduce a saturation scale $Q_s^2(x)$ related with the gluon distribution:

$$\frac{4}{\sigma_0} \frac{\pi^2}{3} \alpha_s x g(x, Q_s^2(x)) = Q_s^2(x) \quad (6)$$

and take

$$Q_s^2(x) = Q_c^2 \left(\frac{x_c}{x} \right)^\lambda, \quad (7)$$

where x_c is a cut-off value of x . We consider low- x gluons to be gluons which carry momentum fraction $x < x_c$. We take $\lambda = 0.29$ from GBW and $x_c = 0.01$ from Stařto et al. analyses. Eqs. (6) and (7) show that as $x \rightarrow 0$, $x g(x, Q_s^2(x))$ increases rapidly as $x^{-\lambda}$. Q_c^2 is phenomenologically determined from the relation $Q_c^2 x_c^\lambda = Q_0^2 x_0^\lambda$ of GBW. σ_0 in Eq. (6) is a cross section, which is identified below. Using Eq. (6) in Eq. (5), we obtain

$$\sigma_{tot}^{dipole}(x, r^2) = 2 \int d^2b [1 - \exp(-r^2 \frac{\sigma_0}{4} Q_s^2(x) \frac{1}{2} f(b))]. \quad (8)$$

If we now take the view that the dipole sees the low- x gluon cloud of a proton as a black disk, then $f(b) = (\pi R^2)^{-1} \theta(R - b)$, where R is the black disk radius. Identifying σ_0 as the black disk cross section, $\sigma_0 = 2\pi R^2$, Eq. (8) becomes

$$\begin{aligned}\sigma_{\text{tot}}^{\text{dipole}}(x, r^2) &= 2 \int d^2b \left[1 - \exp\left(-\frac{1}{4} r^2 Q_s^2(x) \theta(R - b)\right) \right] \\ &= \sigma_0 \left[1 - \exp\left(-\frac{1}{4} r^2 Q_s^2(x)\right) \right],\end{aligned}\quad (9)$$

which is the total dipole cross section in GBW model.

Deep-elastic pp scattering in our model, as we mentioned earlier, originates from deep-elastic valence quark-quark scattering. To describe the low- x gluons around a valence quark, we use Eqs. (6) and (7) of the GBW model, which encode two key premises of the model: namely, how the gluon distribution is related with the saturation scale $Q_s^2(x)$ and how that scale rises sharply as $x \rightarrow 0$. However, we drop the premise that the b -plane distribution of low- x gluons (around a valence quark in our case) can be approximated by a $\theta(R - b)$ function, i.e. by a black disk of fixed radius R . Our reason can be simply seen by examining Eq. (8) for a small dipole traversing the low- x gluon field of a proton at very large dipole-proton c.m. energy ($1/x \rightarrow \infty$). If $f(b)$ falls off as e^{-mb} for large b , then the exponent in Eq. (8) leads to a black disk behavior with a radius $b_{\text{BD}} = (\lambda/m) \ln(1/x)$ and $\sigma_{\text{tot}}(x, r^2) \sim \ln^2(1/x)$, which saturates the Froissart-Martin (FM) bound. On the other hand, Eq. (9) shows that for $f(b) \sim \theta(R - b)$ in the GBW model with R constant, $\sigma_{\text{tot}}(x, r^2) \rightarrow \sigma_0$ (a constant) as $1/x \rightarrow \infty$. The latter does not meet the expected saturation of the FM bound based on analyticity and unitarity [8,9]. Also, numerical investigation of the QCD nonlinear evolution equation by Gotsman et al. shows that $f(b)$ falls off as e^{-mb} for large b , when they exclude the kinematical region of large dipoles [10].

To address the above problem in the context of our valence quark-quark scattering at large \hat{s} (Fig. 2), we require the low- x gluons of a valence quark to have a b -plane distribution $f(b)$, such that: 1) $f(b)$ falls off as e^{-mb} for large b , 2) has finite value at $b = 0$, and 3) satisfies the normalization condition $\int d^2b f(b) = 1$. When \hat{s} is truly asymptotic, the full unitarized amplitude $\hat{T}(\hat{s}, t)$ comes in, leads to a black disk with a radius growing as $\ln \hat{s}$ and a total cross section $\sigma_{\text{tot}}(\hat{s}) \propto \ln^2 \hat{s}$ that saturates the FM bound.

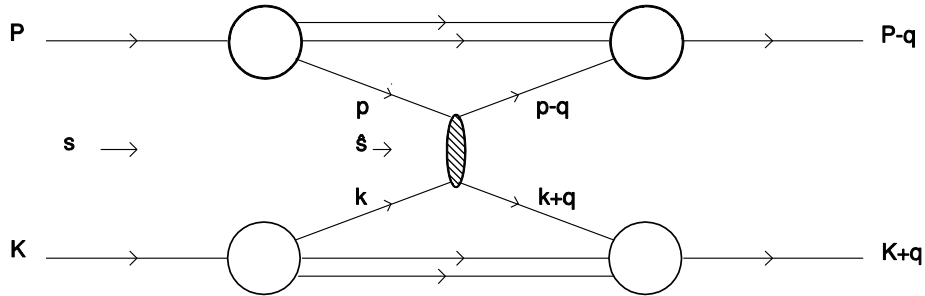


Fig. 2. Hard collision of a valence quark from one proton with a valence quark from the other proton.

We first derive the total cross section in Born approximation for valence quark-quark scattering as shown in Fig. 2. Since the number of gluons for a valence quark lying between momentum fraction x and $x + dx$ and in an area d^2b at a distance b from its center is $dx g(x, Q_s^2(x)) d^2b f(b)$, the cross section in Born approximation (single scattering) for the two colliding valence quarks can be written as

$$\begin{aligned}\hat{\sigma}_B(\hat{s}) &= \int d^2b \int_0^{x_c} dx_1 g(x_1, Q_s^2(x_1)) \int d^2b_1 f(b_1) \int_0^{x_c} dx_2 g(x_2, Q_s^2(x_2)) \\ &\quad \times \int d^2b_2 f(b_2) \tilde{\sigma}(x_1 x_2 \hat{s}) \delta^{(2)}(\vec{b} + \vec{b}_1 - \vec{b}_2).\end{aligned}\quad (10)$$

Here $\tilde{\sigma}(x_1 x_2 \hat{s})$ is an effective gluon-gluon cross section of a gluon carrying light-cone momentum fraction x_1 of one valence quark and a colliding gluon carrying light-cone momentum fraction x_2 of the other valence quark (Fig. 2). \hat{s} is the square of the c.m. energy of the valence quarks: $\hat{s} = (p + k)^2 \simeq p_+ k_-$. From Eqs. (6) and (7), we have $x g(x, Q_s^2(x)) = C (x_c/x)^\lambda$, where C is a constant. $\hat{\sigma}_B(\hat{s})$ can now be written as

$$\begin{aligned} \hat{\sigma}_B(\hat{s}) &= C^2 \int_0^{x_c} \frac{dx_1}{x_1} \left(\frac{x_c}{x_1}\right)^\lambda \int_0^{x_c} \frac{dx_2}{x_2} \left(\frac{x_c}{x_2}\right)^\lambda \tilde{\sigma}(x_1 x_2 \hat{s}) \\ &\quad \times \int d^2b \int d^2b_1 f(b_1) \int d^2b_2 f(b_2) \delta^{(2)}(\vec{b} + \vec{b}_1 - \vec{b}_2) \end{aligned} \quad (11a)$$

$$= \sigma_{\text{gg}}(\hat{s}) \int d^2b F(b). \quad (11b)$$

$\sigma_{\text{gg}}(\hat{s})$ is the gluon-gluon cross section obtained by integrating over low- x gluon densities of the colliding valence quarks. $F(b)$ is the overlap of the gluon densities in the b -plane:

$$F(b) = \int d^2b_1 f(b_1) \int d^2b_2 f(b_2) \delta^{(2)}(\vec{b} + \vec{b}_1 - \vec{b}_2). \quad (12)$$

Comparing Eq. (11b) with Eq. (3), we notice

$$2 \hat{\chi}_1(\hat{s}, b) = \sigma_{\text{gg}}(\hat{s}) F(b). \quad (13)$$

Furthermore, Eq. (12) shows $\int d^2b F(b) = 1$, so that from Eq. (11b) $\hat{\sigma}_B(\hat{s}) = \sigma_{\text{gg}}(\hat{s})$. Using Eqs. (1) and (13), we find the q-q scattering amplitude to be

$$\hat{T}(\hat{s}, t) = i \hat{p} \hat{W} \frac{1}{2\pi} \int d^2b e^{i \vec{b} \cdot \vec{q}} [1 - \exp(-\frac{1}{2} \sigma_{\text{gg}}(\hat{s}) F(b))] \quad (14)$$

and the Born amplitude

$$\hat{T}_B(\hat{s}, t) = i \hat{p} \hat{W} \sigma_{\text{gg}}(\hat{s}) \frac{1}{4\pi} \int d^2b e^{i \vec{b} \cdot \vec{q}} F(b). \quad (15)$$

Defining the low- x gluon form factor of a valence quark by $\hat{f}(q)$:

$$\hat{f}(q) = \int d^2b e^{i \vec{b} \cdot \vec{q}} f(b), \quad (16)$$

we obtain from Eq. (15)

$$\hat{T}_B(\hat{s}, t) = i \hat{p} \hat{W} \sigma_{\text{gg}}(\hat{s}) \frac{1}{4\pi} \hat{f}^2(q). \quad (17)$$

For \hat{s} large, evaluation of $\sigma_{\text{gg}}(\hat{s})$ given by Eqs. (11a,b) leads to the result $\sigma_{\text{gg}}(\hat{s}) \sim \hat{s}^\lambda \ln \hat{s}$. Since the power of λ is not precisely known, we drop the $\ln \hat{s}$ term and write Eq. (17) as

$$\hat{T}_B(\hat{s}, t) = i \hat{s} \gamma_{\text{gg}} \hat{s}^\lambda \hat{f}^2(q), \quad (18)$$

where γ_{gg} is a real positive constant. Requiring $\hat{T}_B(\hat{s}, t)$ to be crossing even, i.e. high energy elastic valence qq and q \bar{q} scattering to be the same, modifies Eq. (18) to

$$\hat{T}_B(\hat{s}, t) = i \hat{s} \gamma_{\text{gg}} \left(\hat{s} e^{-i\frac{\pi}{2}}\right)^\lambda \hat{f}^2(q). \quad (19)$$

We next choose a general form for the low- x gluon distribution in the b -plane:

$$f(b) = \frac{1}{2\pi} \frac{m^2}{\Gamma(\mu+1)} \left(\frac{mb}{2}\right)^\mu K_\mu(mb), \quad (\mu > 0) \quad (20)$$

which satisfies the three conditions we require of $f(b)$. Correspondingly, Eq. (19) becomes

$$\hat{T}_B(\hat{s}, t) = i \hat{s} \gamma_{\text{gg}} \left(\hat{s} e^{-i\frac{\pi}{2}}\right)^\lambda \frac{1}{\left(1 + \frac{q^2}{m^2}\right)^{2(\mu+1)}} \quad (\text{for low-}x \text{ gluons}). \quad (21)$$

As we mentioned earlier, previously we investigated valence quark-quark scattering where the valence quarks interacted via the hard pomeron, i.e. BFKL pomeron (reggeized gluon ladders) plus its next to leading order corrections [7]. Because of significant leading order corrections, the power of \hat{s} : \hat{s}^ω with $\omega = \omega_{\text{BFKL}}$ is substantially reduced to $\omega \simeq 0.13 - 0.18$ as argued by Brodsky et al.[11]. The Born amplitude we used was

$$\hat{T}_{\text{B}}(\hat{s}, t) \simeq i \hat{s} \gamma_{\text{hp}} (\hat{s} e^{-i\frac{\pi}{2}})^\omega \left(1 + \frac{q^2}{m_h^2}\right) \quad (\text{for the hard pomeron}) \quad (22)$$

($m_h = r_0^{-1}$, $\gamma_{\text{hp}} = \gamma_{\text{qq}}/m_h^2$ using earlier notation). Comparing Eqs. (21) and (22), we notice that the structure of the two Born amplitudes are the same. This enables us to carry out present quantitative calculations the same way as before [7]. pp elastic scattering amplitude originating from the valence q-q scattering amplitude (Eq. (21)) is

$$T_{\text{qq}}(s, t) = i s \gamma_{\text{gg}} \left(s e^{-i\frac{\pi}{2}}\right)^\lambda \frac{\mathcal{F}^2(q_\perp, \lambda)}{\left(1 + \frac{q^2}{m^2}\right)^{2(\mu+1)}}, \quad (23)$$

where $s = (P + K)^2$ is the square of the c.m. energy of pp scattering (Fig. 2) and $\mathcal{F}^2(q_\perp, \lambda)$ are structure factors that arise when the momentum distributions of the colliding valence quarks inside protons are folded in. Physically, each structure factor stems from the confinement of valence quarks inside the proton.

Our predicted pp $d\sigma/dt$ at LHC at $\sqrt{s} = 14$ TeV for the whole momentum transfer range $|t| = 0 - 10$ GeV² due to the combined diffraction, ω -exchange, and single hard q-q scattering from low-x gluons is shown by the solid line in Fig. 3. Also shown in the figure are $d\sigma/dt$ due to each of these three processes separately. As before, the parameters of the model were required to provide good fits of $\bar{p}p$ $d\sigma/dt$ at $\sqrt{s} = 546$ GeV, 630 GeV and 1.8 TeV as well as satisfactory descriptions of $\sigma_{\text{tot}}(s)$ and $\rho(s)$ as a function of \sqrt{s} . In our present calculations, the parameters m and μ of Eq. (21) have the values $m = 1.67$ GeV, and $\mu = 1/4$, while the parameter λ responsible for the sharp rise of low-x gluon density has the value $\lambda = 0.29$ as given by GBW.

High energy pp scattering originating from valence quark-quark scattering has also been discussed by Kovner and Wiedemann [12] in a model where the proton is taken as a loosely bound state of three valence quarks. At some initial high energy, they view each valence quark as a black (i.e. totally absorbing) disk with a gray periphery. The black disk originates from saturated gluon density in the central region of a valence quark, while the gray periphery is due to the long range Coulomb-like field of massless gluons. In valence q-q scattering, the interaction between the two gray regions leads to a power like growth of the total cross section and in their model explains the pre-asymptotic behavior of $\sigma_{\text{tot}} \simeq 21.70 s^{0.0808}$ due to the soft pomeron [13]. With increasing s , the black central region of each valence quark grows in transverse size. Comparing the valence q-q scattering in KW model with that of ours, we notice that in our model it is the interaction of the low-x gluons of a valence quark with those of the other in the b -plane (Eq. (11a)), which leads to a power like growth of the Born cross section $\sigma_{\text{gg}}(\hat{s}) \sim \hat{s}^\lambda$; here λ measures the rapid growth of the gluon density ($x g(x, Q_s^2(x)) \sim x^{-\lambda}$). When unitarized using the eikonal description (Eq. (14)), the power growth of the cross section will be tamed at asymptotic \hat{s} by the nonperturbative exponential fall-off of $F(b) \sim e^{-mb}$ and will lead to a black disk of radius $b_{\text{BD}} \simeq (\lambda/m) \ln(\hat{s}/s_0)$ and $\sigma_{\text{tot}}(\hat{s}) \simeq 2\pi [(\lambda/m) \ln(\hat{s}/s_0)]^2$. Furthermore, the black disk will have an outer gray boundary region where the profile function $\hat{\Gamma}(\hat{s}, b) = 1 - \exp(-\hat{\chi}_1(\hat{s}, b))$ falls from $\hat{\Gamma}(\hat{s}, b) = 1$ ($b < b_{\text{BD}}$) to $\hat{\Gamma}(\hat{s}, b) = 0$ ($b > b_{\text{BD}}$). As \hat{s} increases, the black disk radius will grow in transverse size and the gray region will move outward. Since $f(b) d^2b$ is the probability of a gluon to be in an area d^2b at a distance b from the center of the valence quark (Eq. (11a)), we can

calculate the average size of the low- x gluon cloud surrounding a valence quark in the transverse plane; namely, $\langle b^2 \rangle^{1/2}$ where $\langle b^2 \rangle = \int b^2 f(b) d^2b$. Using the values of the parameters $m = 1.67$ GeV and $\mu = 1/4$ for $f(b)$ (Eq. (20)), we obtain $\langle b^2 \rangle^{1/2} = 0.27$ F, somewhat larger than the 0.2 F size used by KW in their estimate of σ_{tot} , but in agreement with the value 0.3 F suggested by Kopeliovich et al. [14].

High energy pp, $\bar{p}p$ elastic scattering have been quantitatively studied by Block et al. in a QCD-inspired phenomenological model [15]. In the c.m. system, a proton is viewed in their model as a disk in the b -plane with a gluon distribution and a valence quark distribution. Both b -plane distributions are described by dipole form factors. Block et al. envisage gluon-gluon, gluon-quark and quark-quark interactions in elastic scattering, and derive the full scattering amplitude using an eikonal description. Their work has been followed up by Luna et al. [16] who introduce a dynamical gluon mass as an infrared mass scale. Calculation of the Born cross section in these models is similar to ours (Eqs. (11a,b)), since these models incorporate the same low- x behavior of the gluon density. However, these models do not associate low- x gluons with the gluon cloud of a valence quark. Instead, the low- x gluons are taken to belong to the whole proton.

We note that the low- x gluons we are considering are specified at the saturation scale $Q_s^2(x)$ (Eq. (6)) where $Q_s^2(x) = Q_c^2(x_c/x)^\lambda$ (Eq. (7)). In the phase space plot: $\ln(1/x)$ versus $\ln Q^2$, gluons lying in the region bounded by the saturation line $\ln Q^2 = \ln Q_s^2(x)$ and the line $\ln Q^2 = \ln Q_c^2$ (separating the nonperturbative regime from the perturbative regime) are referred to as forming Color Glass Condensate (CGC) [17]. The low- x gluons in our calculations, therefore, lie on the boundary of the CGC region. The CGC region, however, can be extended further in $\ln Q^2$ using geometric scaling; namely, $Q^2 \leq Q_{\text{ge}}^2(x)$, $Q_{\text{ge}}^2(x) = Q_s^2(x)[Q_s^2(x)/Q_c^2]^{0.34}$ [17]. As a consequence, the low- x gluons we are considering actually lie well within the CGC region and the low- x gluon cloud around a valence quark can be identified as Color Glass Condensate. Deep-elastic valence quark-quark scattering is then due to Color Glass Condensate around one valence quark strongly interacting with that of the other.

Our predicted pp elastic $d\sigma/dt$ at LHC at c.m. energy 14 TeV and $|t| = 0 - 10$ GeV² shown in Fig. 3 reflects the structure of the proton given in Fig. 1. In the small $|t|$ region, the outer cloud of one proton interacts with that of the other giving rise to diffraction scattering. In the intermediate $|t|$ region (1 GeV² $\lesssim |t| \lesssim 4$ GeV²), one proton probes the baryonic charge density of the other proton via vector meson ω exchange. In the large $|t|$ region (4 GeV² $\lesssim |t| \lesssim 10$ GeV²), one proton scatters off the other proton via a single hard valence quark-quark collision (Fig. 2). The valence quark-quark collision underlying Fig. 3 originates from the low- x gluon cloud of one valence quark strongly interacting with that of the other. An alternative mechanism, studied previously, is the valence quark-quark collision due to the hard pomeron exchange[7]. Both hard q-q scattering processes predict smooth decrease of $d\sigma/dt$ in the large $|t|$ region. pp elastic $d\sigma/dt$ calculations have also been carried out for the whole $|t|$ region $0 - 10$ GeV² using Block et al. model as well as other models [18-20]. All these models predict visible oscillations as well as much smaller cross sections than ours in the large $|t|$ region (Fig. 4). Therefore, precise measurement of elastic $d\sigma/dt$ at large $|t|$ by the TOTEM group will be able to distinguish between our model and the other models and shed light on the dynamics of deep-elastic pp scattering.

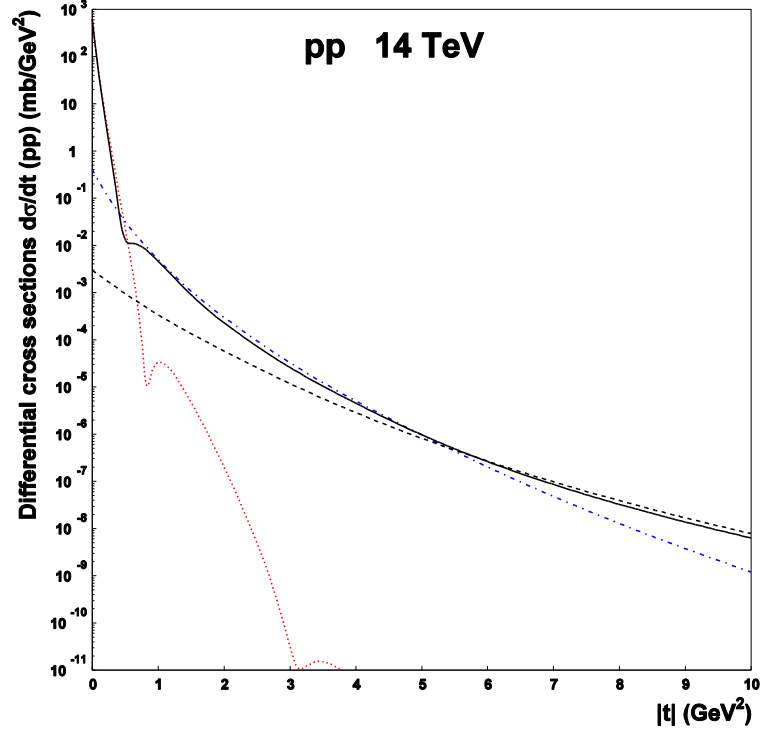


Fig. 3. Solid curve shows our predicted pp elastic $d\sigma/dt$ at LHC at $\sqrt{s} = 14$ TeV and $|t| = 0 - 10$ GeV² from combined diffraction, ω exchange and a single hard valence quark-quark collision due to their low-x gluon clouds. Dotted curve shows $d\sigma/dt$ due to diffraction only, dot-dashed curve that due to ω exchange only, and the dashed curve shows $d\sigma/dt$ from the valence quark-quark collision only.

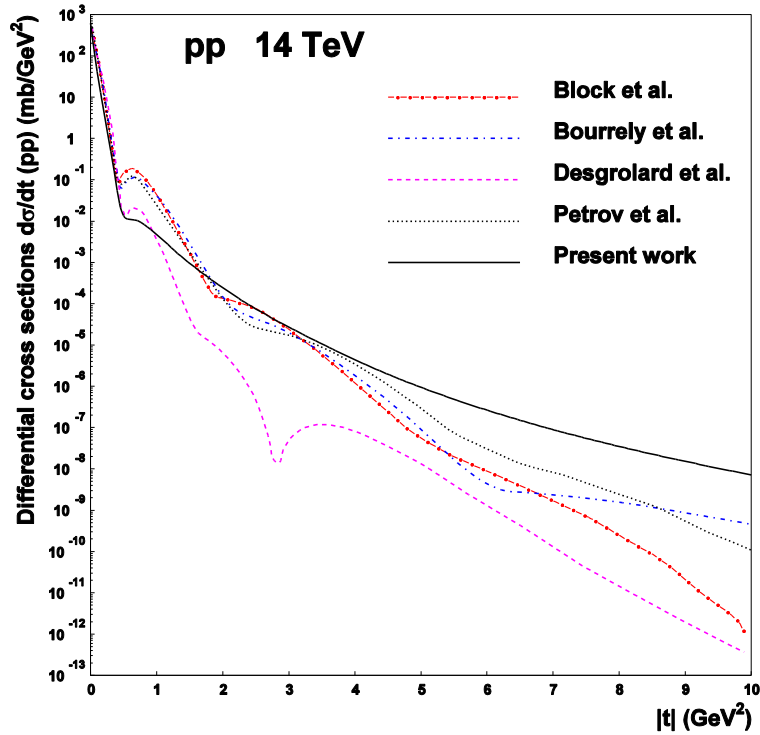


Fig. 4. Comparison of our predicted $d\sigma/dt$ (solid curve) at $\sqrt{s} = 14$ TeV with the $d\sigma/dt$ predicted by Block et al. [15], Bourrely et al. [18], Desgrolard et al. [19], and Petrov et al. (3 pomerons) [20] models.

Acknowledgment

One of us (M.M.I.) would like to thank his colleague Alex Kovner for discussions.

References

- [1] R. D. Heuer, A. Wagner, CERN COURIER **48** (2008) 34.
- [2] K. Golec-Biernat, M. Wüsthoff, Phys. Rev. D **59**, (1998) 014017; **60** (1999) 114023.
- [3] A. M. Staśto, K. Golec-Biernat, J. Kwieciński, Phys. Rev. Lett. **86** (2001) 596.
- [4] TOTEM: Technical Design Report, January 2004, CERN-LHCC-2004-002.
- [5] M. Deile (TOTEM Collaboration), Proceedings of the 12th Int. Conf. on Elastic and Diffractive Scattering (2007), edited by J. Bartels, K. Borras, M. Diehl, H. Jung (to be published).
- [6] M. M. Islam, R. J. Luddy, A. V. Prokudin, Int. J. of Mod. Phys. A **21** (2006) 1.
- [7] M. M. Islam, R. J. Luddy, A. V. Prokudin, Phys. Lett. B **605** (2005) 115.
- [8] M. Froissart, Phys. Rev. **123** (1961) 1053.
- [9] A. Martin, Nuovo Cimento **A42** (1966) 930; L. Lukaszuk, A. Martin, Nuovo Cimento **A52** (1967) 122.
- [10] E. Gotsman, M. Kozlov, E. Levin, U. Maor, E. Naftali, Nucl. Phys. A **742** (2004) 55.
- [11] S. J. Brodsky, V. S. Fadin, V. T. Kim, L. N. Lipatov, G. B. Pivovarov, JETP Lett. **70** (1999) 155.
- [12] A. Kovner, U. A. Wiedemann, Phys. Rev. D **66** (2002) 034031.
- [13] A. Donnachie, P. V. Landshoff, Phys. Lett. B **437** (1998) 408.
- [14] B. Z. Kopeliovich, I. K. Potashnikova, B. Povh, E. Predazzi, Phys. Rev. D **63** (2001) 054001.
- [15] M. M. Block, E. M. Gregores, F. Halzen, G. Pancheri, Phys. Rev D **60** (1999) 054024.
- [16] E. G. S. Luna, A. F. Martini, M. J. Menon, A. Mihara, A. A. Natale, Phys. Rev. D **72** (2005) 034019.
- [17] For a recent review of the field, see J. Jalilian-Marian, Y. V. Kovchegov, Progress in Particle and Nucl. Phys. **56** (2006) 104.
- [18] C. Bourrely, J. Soffer, T. T. Wu, Eur. Phys. J. C **28** (2003) 97.
- [19] P. Desgrolard, M. Giffon, E. Martynov, E. Predazzi, Eur. Phys. J. C **16** (2000) 499.
- [20] V. Petrov, E. Predazzi, A. V. Prokudin, Eur. Phys. J. C **28** (2003) 525.